JOURNAL OF GEOPHYSICAL RESEARCH, VOL. 111, D03303, doi:10.1029/2005JD006086, 2006

Apportionment of black carbon in the South Shetland Islands, Antarctic Peninsula

Enio Bueno Pereira
Center for Weather Forecasts and Climate Studies, National Institute for Space Science, Cachoeira Paulista, São Paulo, Brazil

Heitor Evangelista and Kely Cristine Dalia Pereira
Laboratory of Radioecology and Global Change, State University of Rio de Janeiro, Rio de Janeiro, RJ, Brazil

Iracema F. A. Cavalcanti and Alberto W. Setzer
Center for Weather Forecasts and Climate Studies, National Institute for Space Science, Cachoeira Paulista, São Paulo, Brazil

Received 25 April 2005; revised 24 August 2005; accepted 11 October 2005; published 10 February 2006.

[1] Simultaneous time series measurements of black carbon (BC), aerosol particle number (ANC), radon, and SEM-EDS analysis for total carbon were collected at the Brazilian Antarctic station Ferraz, northwest of the Antarctic Peninsula (62°05′S, 58°23.5′W) for the years of 1993, 1997, and 1998. A new data screening technique was applied in an effort to distinguish long-range from local contaminations of BC. Analyses of data revealed a small increase in BC concentration during winter-to-spring seasons. The mean annual BC concentration of 8.3 ng m^{-3} was consistent with global model estimates for this region. The intermittent coupling mechanism between the regional circulation of the low-level jets and the passages of the frontal systems explained the transport of BC from areas of burning biomass in Brazil to the northern Antarctic Peninsula. Principal component analysis applied to BC, Radon, ANC, and meteorological data presented significant factor loadings linking BC with ^{222}Rn and with wind velocity corroborating with this hypothesis.

Citation: Pereira, E. B., H. Evangelista, K. C. D. Pereira, I. F. A. Cavalcanti, and A. W. Setzer (2006), Apportionment of black carbon in the South Shetland Islands, Antarctic Peninsula, *J. Geophys. Res.*, *111*, D03303, doi:10.1029/2005JD006086.

1. Introduction

[2] Aerosol black carbon (BC), also known as graphitic carbon, elemental carbon, or soot, is usually linked to anthropogenic activities such as fossil fuel combustion, mostly restricted to urban areas, power plants, and industries and to vegetation fires triggered both from natural and manmade causes. It has been employed to trace atmospheric transport of urban pollutants in remote atmospheres [*Hansen et al.*, 1988; *Murphey and Hogan*, 1992]. Vegetation fires also constitute a significant source of BC particularly in the Southern Hemisphere tropical regions. Estimates made by *Penner et al.* [1993] based on regional BC to SO_2 inventory ratios indicate about 5×10^{12} g of C per year of the BC emissions to the atmosphere originate from South America and Africa together, that is 94% of their estimated global biomass burning emissions.

[3] BC is a major light absorbing aerosol component in the atmosphere. Light absorption efficiencies of smoke particles from biomass fires (average of 12.1 m^2/g) was estimated by *Martins et al.* [1998] during the SCAR-B (Smoke, Clouds, and Radiation-Brazil) campaign in the Amazon and Cerrado region during August–September 1995. It has been linked to climate changes issues in several studies [*Hansen and Nazarenko*, 2004; *Satheesh and Ramanthan*, 2000; *Penner and Zhang*, 2003]. Estimates of direct forcing by BC from fossil fuel combustion ranges from 0.16 to >0.5 W/m^2 [*Intergovernmental Panel on Climate Change*, 2001; *Jacobson*, 2002]. According to *Penner and Zhang* [2003], soot and smoke aerosols that contain BC may offset the negative climate forcing of anthropogenic aerosols by absorbing radiation. *Sato et al.* [2003] using AERONET data with a global aerosol computer model found that the amount of sunlight absorbed by BC was two to four times larger than previously recognized.

[4] The large light absorption characteristics of BC may also cause indirect effects on climate. *Hansen and Nazarenko* [2004] have estimated a climate forcing effect of 0.3 W/m^2 by soot on high-latitude snow and ice albedoes of the Northern Hemisphere. According to the study, the calculated global warming from soot in snow and ice for a 120-year simulation could account for 25% of the observed global warming.

[5] For *Battye et al.* [2002], major worldwide anthropogenic sources of BC are split evenly with coal and diesel combustion accounting for approximately 50% of emissions. *Cooke and Wilson* [1996] reported their results of a three-dimensional model for BC transport by using a global inventory of BC worldwide and found that biomass burning emissions are roughly 33% lower than that from fossil fuel combustion. The widespread influence of the biomass

0148-0227/06/2005JD006086$09.00

combustion products has been identified in several occasions at sites relatively far from their sources. For example, *Fishman et al.* [1990] attributed the observed enhancements of trace gas concentrations in Ascención Island in the Atlantic Ocean (8°S; 015°W) to the emissions from biomass burning in central Africa and, to a lesser extent, in South America. In pristine and remote atmospheres, such as over the Antarctica, the very few studies thus far are not conclusive with regard to source terms and associated synoptic meteorological transport [*Murphey and Hogan*, 1992].

[6] *Setzer and Pereira* [1991a] indicated the transport of emissions from the 1987 vegetation fires in the Amazon to Antarctic latitudes after examining images from satellites and tropospheric flow charts. *Wolff and Cachier* [1998] measured the seasonal cycle of BC at Halley Antarctic station (75°S; 26.7°W) and reported a marked overall maximum of about 12 ng m^{-3} in October superimposed on the monthly average values of 0.3–2 ng m^{-3}. According to their interpretation this pattern seemed to be controlled by the timing of biomass burning in the tropics.

[7] *Muñoz et al.* [2004] have suggested that low-level winds could account for the long-distance dispersal of several biotic species and precursors (seeds, pollen, spores, etc.) in the Southern Hemisphere. Their analysis was based on the study of direction-dependent long-distance dispersal by wind and floristic affinities among landmasses and showed that South American aerosol particles species can reach the Malvinas/Falkland islands.

[8] In contrast to the meso-to-large scale advective transport concept, the local impact of fossil fuel burning by electricity energy power plants and by powered vehicles in Antarctic research stations have also been addressed in the literature [*Warren and Clarke*, 1990], indicating that they must be taken into account in interpreting the BC data for global studies.

[9] *Pereira et al.* [1988] and *Pereira* [1990] studied the advection of continental air from South America in the troposphere of the Antarctic Peninsula by the use of ^{222}Rn tracer and demonstrated that synoptic-scale transport of continental trace components in the atmosphere can be explained by the presence of cyclonic systems that move eastward through the Drake Passage at latitudes close to 60°S. Using ^{222}Rn as the reference tracer, *Jacob et al.* [1997] verified that global chemical transport models can explain the observed radon concentrations measured by *Pereira* [1990] in the north of the Antarctic Peninsula. Source terms of radon for these model runs were located mainly in South America and Africa, calling attention to the importance of the meridional exchange of chemical species in the troposphere at higher latitudes in the Southern Hemisphere.

[10] *Pereira* [2002] and *Pereira et al.* [2004], employing SEM-EDS microanalysis of insoluble particulates from a deep ice core from King George Island/South Shetland Archipelago and in the Chilean Patagonia atmosphere found out that 95% of continental dust in the north of the Antarctic Peninsula could be explained by the atmospheric transport from Patagonia.

[11] A study carried out by *Basile et al.* [1997] studying the origin of airborne aerosol particles trapped in the ice of Central Antarctic Plateau at Vostok (78.5°S; 106.9°E) and "Dome C" (South Pole) stations concluded that the Patagonian region was the most probable source of aerosols in continental Antarctica. That study was based on stable isotopes measurements of Nd and Sr. In a related recent study of source regions for dust in east Antarctic during the recent glacial maxima *Smith et al.* [2003] concluded that loess from north of about 35–37°S cannot contribute significantly to dust in Antarctic ice cores.

[12] In Brazil, BC and several other pollutants linked to industrial-urban activities in large cities (population above ~6 million inhabitants) exhibit seasonal variation with maximum concentrations during the austral winter (June, July, and August), and minimum during summer (December, January, and February) [*Maldonado*, 2003]. This is mainly associated to the wintertime inversion of the temperature profile in the lower troposphere and, to a minor extent, also to the subsidence of the tropopause and to low overall rainfall. The other important source term of BC is the induced burning of native vegetation, mostly to create and renew pasture and agriculture land areas. Secondary vegetation and pastures are also commonly burned at a rate of once every 3 to 4 years. This practice is mostly restricted to the dry season and concentrates from through October in central South America, becoming more intense in El Niño years.

[13] In South America the plume of biomass burning products outflows southeastward to the Atlantic Ocean, mostly in the coastal region located somewhere in south Brazil and north Uruguay, depending on the location of the cold fronts and the tropical jet stream associated to the large subtropical cyclones. *Pereira et al.* [1996], *Anderson et al.* [1996], and *Artaxo et al.* [1998] reported direct measurements of this outflow in several occasions.

[14] *Maldonado* [2003] reported a study of BC and ANC performed in a remote coastal area in southeast Brazil, at "Ilha Grande" (22°11′S; 044°12′W) which showed a bimodal distribution in the BC time series during winter (June through September) and suggested two independent sources in the outflow: fossil fuel and biomass burning. A combination of meteorological conditions and emission rates produce an enrichment of black carbon in aerosols during the period June–October and a reduction during November–May in central South America. Most often, BC derived from burning biomass and fossil fuel combustion mix within the plume along its trajectory, making it difficult to distinguish between theses two contributions in aged plumes. This is the case for the measurements performed in remote sites, such as in the Antarctic continent, when an unequivocal signature for the two possible origins of BC is required. *Evangelista and Pereira* [1994] studied the local atmospheric contamination with BC at King George Island based on observations of sudden simultaneous increases of aerosol particles and BC during periods of more intense local human activities, such as the transit of motorized vehicles and occasional visits of aircrafts and ships.

[15] Figure 1 depicts a compilation of BC measurements taken worldwide [*Maldonado*, 2003], including measurements taking in this work. The left side of Figure 1 represents the sites where measurements were obtained with the size of dots proportional to the concentration. The right side is a plot of the concentration change with latitude. The compilation includes both natural and manmade

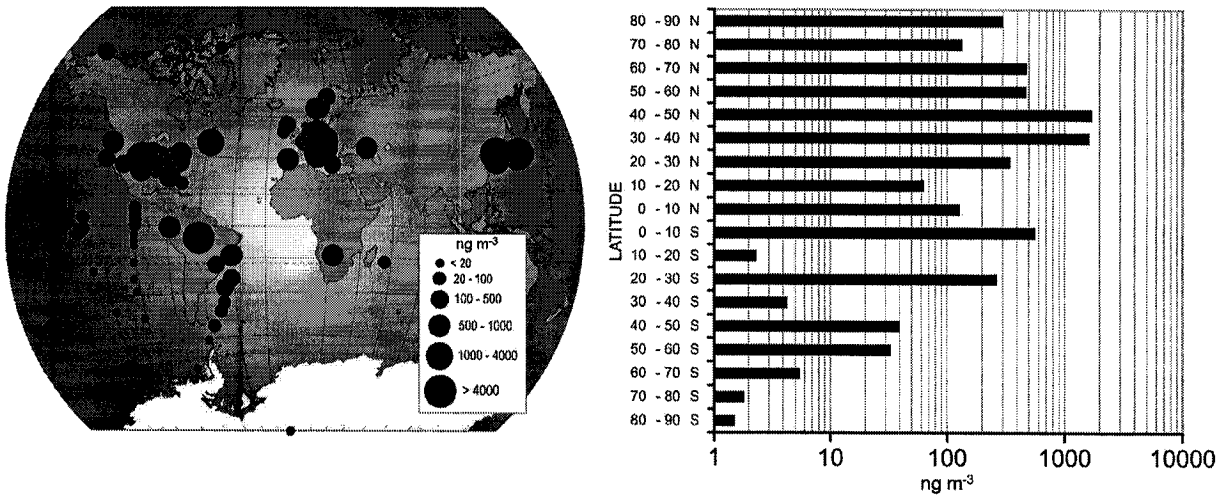

Figure 1. (left) Worldwide BC inventory [*Maldonado*, 2003]; (right) latitudinal average BC concentration.

sources of BC. This compilation shows that south of the equator Brazil and Africa could be considered as major source terms of BC.

[16] We report in this work new results and interpretations for BC concentrations measured at the Brazilian Antarctic station Ferraz for the years of 1993, 1997, and 1998, considering aspects of local versus distant production sources and long-range transport of emissions from vegetation fires in central South America.

[17] Atmospheric monitoring was conducted at the Brazilian Antarctic Research Station "Comandante Ferraz" (62°05′S, 058°23.5′W), located at Admiralty Bay, King George Island, South Shetland Islands, northwest of the Antarctic Peninsula (Figure 2). According to the Köppen classification, the local climate is Polar-Tundra, "ET." Average annual temperature is +1.8°C, with absolute extremes varying from −29°C to 14°C; north to west winds from oceanic air masses prevail (http://www.cptec.inpe.br/antartica/).

[18] Recent measurements of deuterium/hydrogen ratios and ^{3}H in snow, *firn* and ice of a 60 m ice core from the island suggested an average annual precipitation rate of 0.63 m y^{-1} [*Pereira et al.*, 2004] and estimates in the past for the area indicated around 0.4 m y^{-1} [*Schwerdtfeger*, 1970]. The exposed terrain is only a minute fraction of the total ice-covered island area, with less than 1%, distributed mainly along the coastline and steep slopes. A thick ice sheet covers the remaining area of the island, with a maximum thickness of approximately 357 m [*Simões et al.*, 1999]. During winter, snow and ice accumulates, covering most of the summer-exposed terrain. Events of snowmelt occur often in association with rains and positive temperatures of strong cyclonic systems due to the advection of air masses from higher latitudes driven by their warmer sectors. Occasional anticyclone circulation in the region, in all seasons, brings very warm air masses directly from South America, causing temperature rises of up to 20°C and reaching many degrees above zero. Storm tracks derived from satellite images indicate that the strongest eddy activity is located mostly between 30°S and 60°S; however, the density of cyclones around Antarctica at high latitudes is higher than at middle latitudes as shown in a compilation made by *Karoly et al.* [1999].

2. Experimental Methods

2.1. Black Carbon Measurements and Associated Uncertainties

[19] BC was measured at Ferraz in 1993, 1997, and 1998 with an aerosol absorption photometer (aethalometer, model AE9 Magee Inc.). In this method, BC measurements are made by an optical device that continuously measures the

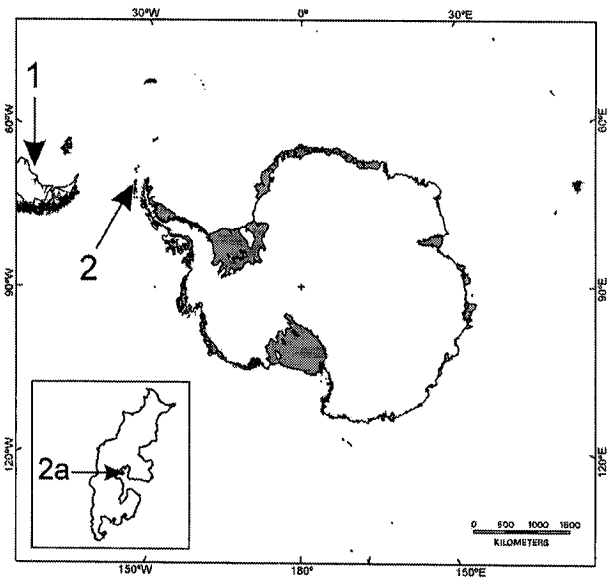

Figure 2. Map of the Antarctic region showing the southern tip of South America (shown by 1 on map) and King George Island (shown by 2 on map), with the location of Ferraz Station (shown by 2a on map) where atmospheric BC measurements were performed between 1992 and 1997.

rate of decrease in the transmissivity of light through a quartz microfiber filter with an effective deposition surface of 0.95 cm^2. This rate of decrease in transmissivity divided by the sampling flow rate is directly proportional to the light absorption coefficient of the aerosols.

[20] The light extinction in the filter, both in the infrared and visible range, is most entirely due to the BC particles in the aerosols due to their large optical absorption. When filters do not contain an abnormally higher quantity of BC or of other dust particle aerosols the light extinction measured in the filters can be directly converted to the BC aerosol mass by a standardized calibration curve [*Hansen and Schnell*, 1991].

[21] In the oceanic atmosphere where the samples were conducted this assumption is particularly valid, since around 94% of total aerosols are composed exclusively by sea salt in the coarse mode, while in the fine mode (below 1 μm) 97% are sea sulfates and sea salt [*Correia*, 1998] with much lower light absorption cross sections as compared to BC.

[22] The sampling system contains a single light source, a low-voltage long-life filament lamp, and two light sensors that detect the black carbon at fixed time intervals. The sensing light beam response due to light intensity variation through the filter is given as the ratio $(SB - SZ)/(RB - RZ)$, [*Hansen and Schnell*, 1991], where *SB* is the sensing beam detector output with lamp on, *SZ* is the sensing beam detector zero offset output with lamp off, *RB* is the reference beam detector output with lamp on, and *RZ* is the reference beam detector zero output with lamp off. The algorithm applied to derive the BC mass concentration from the light intensity readings from the equipment is described next. The attenuation of the light source beam by the filter is given by

$$attn = -100 \ln\left[\frac{(SB - SZ)}{(RB - RZ)}\right]. \quad (1)$$

The increase in the light attenuation is proportional to the increase of surface load of BC on the filter, and the amount of BC in the air stream can be given by

$$[BC] = \frac{S}{\phi \times \sigma_a} \times \frac{\Delta attn}{\Delta t}, \quad (2)$$

where $[BC]$ is the mass concentration of BC, σ_a is the black carbon absorption cross section for visible light, S is the BC-stained area in the filter, and ϕ is the airflow rate through the filter. The aerosol particles deposited on filters never reached the "saturation threshold" when the linear dependency between the aerosol particle concentration and the optical attenuation is no longer valid. In principle, the sampling time interval, Δt in equation (2) should be such that enough BC accumulated in the light sensitive area of the detector during field measurements to yielding statistically significant measurements of BC. Yet this sampling time interval was not known in advance for the Ferraz area. So, we devised a new data acquisition method in which the sampling time interval was set to a very low value (30 min in our case) regardless of the significance of each individual BC value that was obtained by the instrument software in the field. Then we recorded only the raw values for the sensing beams and reference beams and, of course, the time. With this original raw data in hand we repeatedly applied equation (2) at increasing time intervals (known as integration time ≫ sampling time) till we were able to obtain mostly positive values for BC. While applying this method, we also performed a data screening procedure to subtract bad data as described in section 3.

[23] From the above the overall uncertainties concerning the BC data obtained by employing this method lie on the variation of the aerosol deposition area, the flow rate, the sampling time interval, and the attenuation coefficient, which is in a first-order approximation dependent on the absorption cross section and BC concentration. Except for the attenuation coefficient, all other parameters can be precisely controlled by the instrumentation setup. As reported by *Hansen and Schnell* [1991], the aethalometer calibrations were made by comparison with BC concentrations evaluated by a chemical colorimetric technique that makes use of its thermo refractory property. The absorption cross section of the BC is the most significant parameter as far as error sources are concerned, considering that it depends on the aerosol particle aerodynamic radius and density, on the BC internal mixing, and on the BC origin (from burning biomass or fossil fuels) [*Liousse et al.*, 1993]. Values of BC absorption cross section have distinct characteristics according to the sources from urban, rural, or remote areas. The algorithm for BC concentration employs a single value of absorption cross section, σ_a, and thus variations in the BC concentration by the aethalometer may reflect unaccounted variations of σ_a. In addition, atmospheric relative humidity may influence BC measurements, since water accumulates on the filter during the air filtering. The effect of the liquid water on the transparency of the filter collection may be quite important on the final value of BC concentration evaluated by this procedure mainly by affecting the value of σ. Relative humidity is also related to the aerosol particle-growing factor, which shifts σ_a value [*Kirkevag et al.*, 1999]. We estimate that an uncertainty between 10 to 20% occurs only due to these instrumental considerations.

2.2. Aerosol Number Concentration (ANC)

[24] Near real-time ANC measurement was performed together with BC concentration sampling. The goal was to use the ANC data as a quality control for the BC measurements (data screening). A condensation nuclei counter (TSI, CNC-3760) measured the small aerosol particles. This instrument uses a 5 mW laser diode as light source to detect and count small aerosol particles with diameters larger than 0.014 mm over the range of 0 to 104 particles/cm^3 (at 6% coincidence level, factory calibrated). The response time is approximately 2 s at a constant flow rate of 1.4 liter per min. The software from the manufacturer installed on a PC computer connected to the remote processor permitted to program the time interval of sampling. In the case of our experiment this set up time was 10 min. Detailed information regarding its use in marine environment can be obtained in the work of *Maring and Schwartz* [1994].

2.3. Aerosol Particle Elemental Composition

[25] BC-stained microfiber filters from the aethalometer were also submitted to elemental composition analysis and aerosol particle morphology characterization. In this case,

we applied the Scanning Electronic Microscopy (SEM) and the Energy Dispersive Spectrometry (EDS) techniques. Each analyzed filter corresponded to a period of 15 days of continuous sampling. Filters selected for SEM+EDS analysis comprised a complete season period for the year of 1997. The methodology followed *Brian et al.* [1982] and *Petit et al.* [1983] for Antarctic aerosols. Data were available in relative percentage abundance for each detectable element exhibiting values above 1% detection level, for particles with mean diameter above 1 μm. In this work, we report the time variation of total carbon abundance.

3. Protocol for Black Carbon Data Screening

3.1. Local BC Contribution

[26] Several potential anthropogenic sources of BC exist in the Antarctic Peninsula, in particular at King George Island. Therefore a critical examination of the raw data is required to minimize local source interferences on the BC time series. As previously mentioned, sampling time with the aethalometer was set to 30 min in order to select and remove the very rapid BC concentration surges that are typical of local sources. Although this procedure sometimes yielded unreliable individual results owing to poor sampling statistics during data acquisition, the integration of the resulting data set for a larger period after a noise removal procedure described below lead to more reliable results. The most important local source of BC comes from the diesel engines in the electrical power plant of the Brazilian station, distant about 1.6 km from the aethalometer; the nearby Arktowsky station, distant about 10 km from Ferraz is another potential contamination source. Nevertheless, we estimate that these constitute steady sources of BC to the atmosphere since the electric power plants run around the clock all year round. The same hypothesis can be applied for the electric power plants of the other eight stations located on the same King George Island but far more distant.

[27] For the purpose of the present work, we adopted the data screening procedure reported by *Warren and Clarke* [1990] for the South Pole station, where a "dirty" angular sector and a "clean" angular sector were defined comprising the local and the long-range transport contributions. A second important source of BC is linked to the process of burning of organic waste by the local stations. This source is not a steady one and it is quite common, particularly during the summer campaigns in Antarctica when the level of human occupation reaches its maximum. Nevertheless, this procedure occurs at more or less regular intervals of time (weekly at Ferraz) in order to prevent the accumulation of large volumes of biodegradable residues of local impact for the life environment. Furthermore, these events were registered on the field logbook for later data interpretation. The third source is of relatively random nature and it is due to the operation of vehicles powered by fossil fuel. This group includes snowmobiles and other larger land vehicles, small boats, supporting ships, and helicopters, but these events are all registered on the station control logbook.

[28] The larger impact of all these sources combined occur during the station's summer campaign (November through March), when the increased presence of the scientific and technical staff in the station leads to a corresponding increase in activities related to logistics and station maintenance. It is during this same period that the support from vessels and aircrafts operations peak in the area with a consequent increase in the emission of pollutants to the atmosphere.

[29] King George Island has one of the highest human population densities of the entire Antarctic continent. This is true because of the large concentration of research stations and support bases and for its proximity to South America, which facilitates local tourism during summer months. The operation of several scientific stations together and all the logistics associated with them lead to an increase of atmospheric pollution and consequently an increase in background level of black carbon concentration. Because of this fact, it is of prime importance to apply methods to discriminate BC from local contribution and from long-range atmospheric transport. These methods are either based on the study of the isotopic or chemical signature of BC or on the study of the geographical apportionment, using wind direction [*Warren and Clarke*, 1990]. During the winter of 1993, we studied the BC measurements from the point of view of the wind direction and the result is presented in Figure 3 (left). Concentrations were grouped in a 20-degree interval wind rose chart division. The center of the diagram is the sampling point and the numbers represent the scientific stations under operation at that time. The results comprise the period from March to December of 1993. It can be observed that potential local contributions cannot be discarded. The proximity of Ferraz Station from the sampling point explained the higher contribution for BC in the air. The point represented by 8a in Figure 3 (left) is the true geographic location of Ferraz Station while 8b is the virtual location as far as BC is concerned, considering local topographic effect on the surface wind. This virtual position was obtained by simple correlating time series of wind speed and directions from both sites. The expected concentration increase is not very pronounced between 200° and 255°, the angular sector where most of the stations are located. The concentration increases observed between S and SE corresponded to rare events as seen in Figure 3 (left), with little influence to the whole average.

[30] Figure 3 (right) represents the wind rose frequency distribution at Ferraz Station during 1993. Despite the influence of the local topography on low-level winds from the west, it shows that the two most frequent wind directions tend to be in agreement with the local conditions common in most of the frontal systems in the South Shetland Islands. The north wind direction corresponds to the initial phase of cyclonic systems during their trajectory along the Drake Passage, and the SW direction are normally associated to their last step at this region while moving into the Weddell Sea. This same figure shows that the angular sectors corresponding to Ferraz Station (20° to 60°) exhibit high average BC contents but correspond to a relatively small wind frequency as seen in Figure 3 (left).

[31] To avoid "suspicious data" having local origin, several measures and a data screening protocol were established. The sampling site was set away 1600 m from the station's power plant in order to minimize its impact on the BC measured at the sampling point. The protocol registers most events of garbage burning and activities such as transit of motorized vehicles, helicopters, and boats, with the date

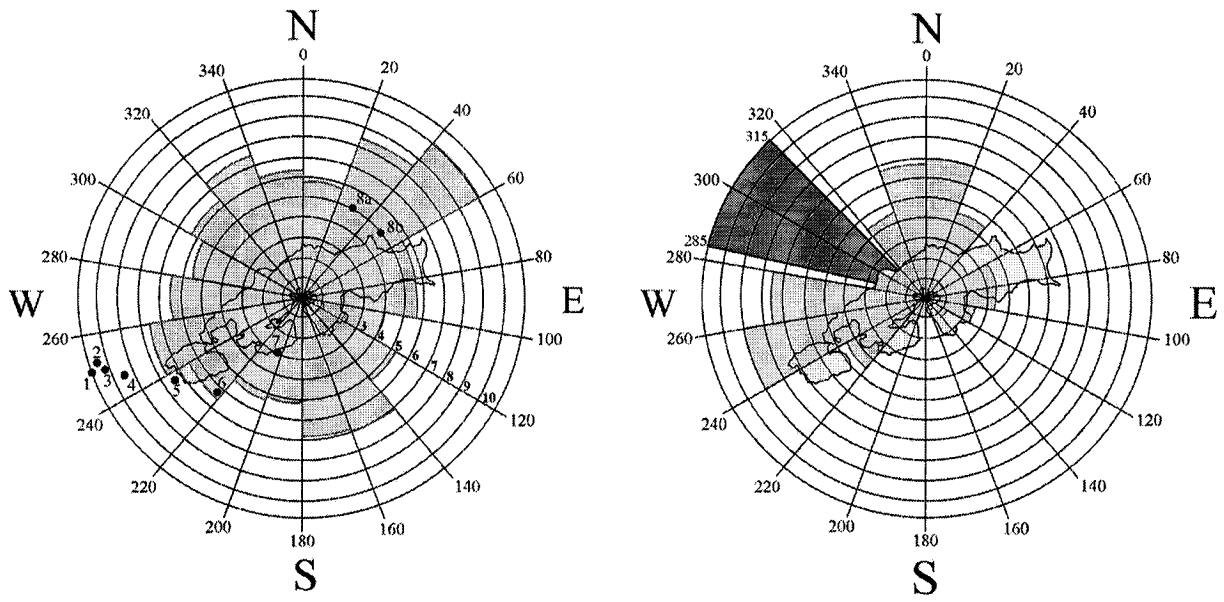

Figure 3. (left) Black Carbon angular distribution frequency around the sampling point (at the center). Data refers to the period of March–December 1993. Each concentric circle interval in radial scale represents 1 ng m^{-3}. Numbers indicate Antarctic Station as follows: (1) Great Wall/China; (2) Frei/Chile; (3) Bellinghousen/Russia; (4) Artigas/Uruguay; (5) King Sejong/South Corea; (6) Jubany/Argentina; (7) Arctowski/Poland; (8a and 8b) Ferraz/Brazil; (right) wind frequency distribution at Ferraz Station, during 1993. Each concentric circle interval in radial scale represents 30 observations. The darker sector between 285° and 315° indicate the region shadowed by local topography (weather source http://www.cptec.inpe.br/antartica/).

and hour of occurrences. In addition, a Condensation Nuclei Counter operating together with the aethalometer also monitored the sampling point in real time in order to characterize the surges of BC. Measurements of ANC respond faster to surges induced by local anthropogenic sources (~2 s response time). Setting up the integration time to 10 min was considered a compromise between the necessary response time and the volume of data to store. This simple data screening procedure functioned satisfactorily. When both BC and ANC time series were plotted together it was possible to tag BC surges of local origin. Thus the data screening was based on a case-by-case exam of the time series and the inspection of the station logbook, a very time-demanding but necessary procedure. Our field observations at King George Island show that surges of local BC have distinct time series signatures in comparison to rises of BC due to long-range transport from central South America. Concentrations of BC associated to long-range air masses displacements increase steadily in time and decrease following almost this same pattern, whereas local black carbon contributions increase rapidly often following an irregular pattern, reaching concentration values of up to two orders of magnitude higher than the annual average. These events were normally attributed to the traffic of snowmobiles, boats, and airplanes in the environs of the sampling point. The corresponding records identified as bad were simply removed from the global database.

[32] Typically, air filters from the aethalometer were changed at 2-week periods, depending on the rate of BC accumulation. Filters were documented and stored under clean conditions on sealed plastic bags for transport back for laboratory analysis in Brazil. The filters were submitted to the SEM-EDS technique for inspection of possible anthropogenic contamination. In this procedure, we searched for enhancements of carbon aerosol particles and associations with metal elements within the individual particle structure. Filters exhibiting high abundance of carbon particles with equivalent diameters of 5 μm or larger were considered candidates for this inspection procedure. Figure 4 illustrates two examples of this analysis for filters presenting gigantic carbon aerosol, one for the summer season (Figure 4a) and the other for the winter season (Figure 4b). In summer, BC particles occurred in association with terrigenous elements, probably due to resuspension of bare soils and particles scoured from rock outcrops as a result of the increase in ice-free areas. During winter, BC particles are predominantly associated with elements of marine origin due to the reduction of the ice-free areas and the consequent increase of the oceanic influence.

3.2. Labeling BC Events With the Help of ^{222}Rn Atmospheric Tracer

[33] *Pereira* [1990] and *Pereira et al.* [1988] explained the origin of radon concentration upsurges at Ferraz Station through synoptic analysis of surface winds, atmospheric pressure, and air temperature along with NOAA satellite images. The surges were linked to the transport of ^{222}Rn-enriched atmosphere from South America during the passage of cyclonic systems through the Shetland Islands. Moreover, *Evangelista and Pereira* [2002] were able to label continental Radon enriched air masses over Ferraz area by applying a model based on the isotopic ratio

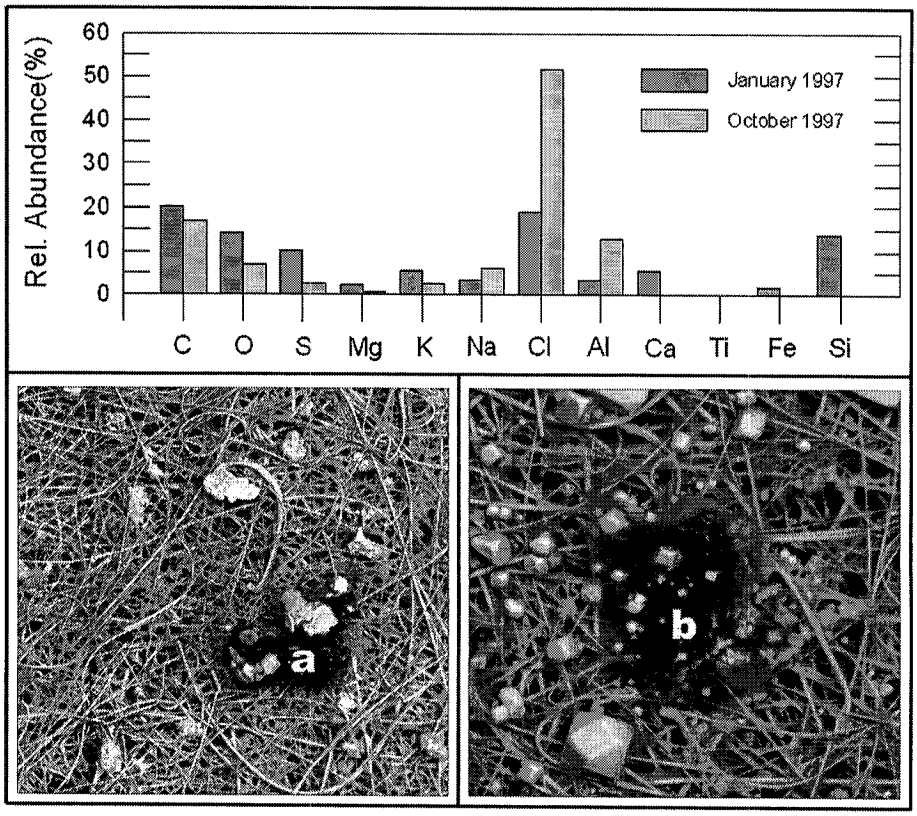

Figure 4. Microphotographies show BC enriched aerosol particles and their relative elemental abundance found in (a) January and (b) October 1997.

$^{220}Rn/^{222}Rn$. One of the best observed cases illustrating this air mass transport from South America to the Antarctic Peninsula with consequent upsurge of ^{222}Rn was observed in June 1997 and is depicted in Figure 5. This figure shows an example of a BC surge from a reported local source (A) with corresponding increases of ANC without the corresponding increase in ^{222}Rn concentration and from a long-range atmospheric transport (B), showing a corresponding increase of ^{222}Rn.

[34] Results of almost 10 years of radon monitoring at Ferraz Station show this good correlation between surges of ^{222}Rn activity concentration and the warm sector of deep cyclonic systems that move eastwards between the Antarctic Peninsula and South America. These surges of ^{222}Rn concentrations are generally not accompanied by corresponding surges of ^{220}Rn, a radioisotope with very short half life (55 s) that traces the local contribution, even during the austral summer when ice-free areas reach their largest extent. This is a strong indication of the long distant origin of the corresponding air masses. During these events, the time series exhibited ^{222}Rn surges of at least three times the average annual activity concentration. Time series for BC may also show events of typical concentrations two to three orders of magnitude higher than the annual BC average and may or may not be related with the ^{222}Rn surges. Furthermore, a basic difference between these two transient behaviors is their duration.

[35] Radon surges often occur in a timescale of 1.5 days while events of local BC growth last typically around a few hours. Simultaneous BC and ^{222}Rn increases where labeled as continental atmospheric transport on account of the preferred continental origin of ^{222}Rn. Simultaneous rises of BC and ANC combined with short duration events with no corresponding ^{222}Rn activity concentration increase was labeled as local anthropogenic.

4. Black Carbon Time Series

[36] BC time series (Figure 6) are not continuous due to several unexpected factors such as instrument failures and others related to the Ferraz station. These interruptions during summer were mostly related to equipment maintenance and/or replacement difficulties. Furthermore, several gaps in the time series were due to the limitations in the occupancy of Ferraz during summer campaigns, which also limits the number of experiments granted for this period. Summer seasons in Ferraz are mostly reserved for field missions in biology and geology. Also, no BC measurements were taken between 1994 and 1996.

[37] Figure 7 shows the monthly averages of BC and ANC. The main feature that can be observed in this figure is a tendency for lower values of BC concentration during the fall-winter seasons and higher values for the spring-summer austral seasons. ANC shows an even more pronounced season effect. It is expected that the fine and coarse aerosol particle modes as well as particle number concentrations have similar behavior [*Correia*, 1998; *Evangelista*, 1998].

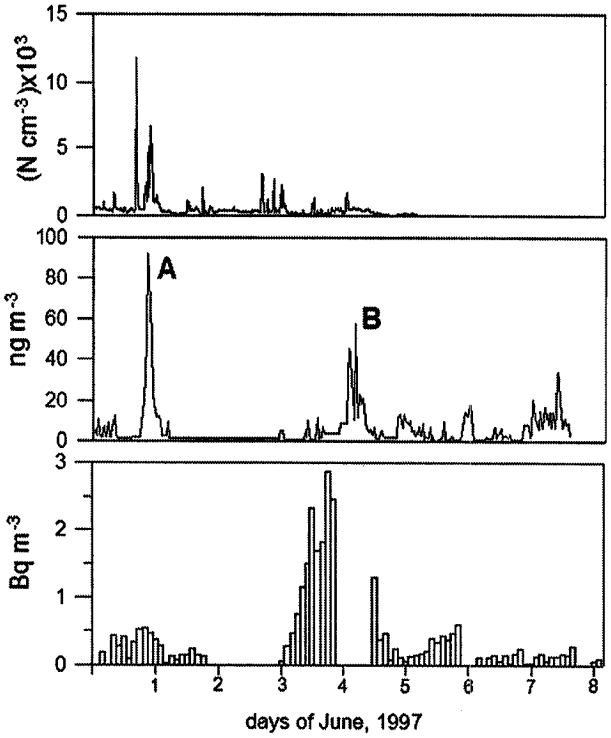

Figure 5. Surges of (bottom) ^{222}Rn, (middle) BC, and (top) ANC. "A" and "B" represent independent events observed at Ferraz Station during winter season (1997).

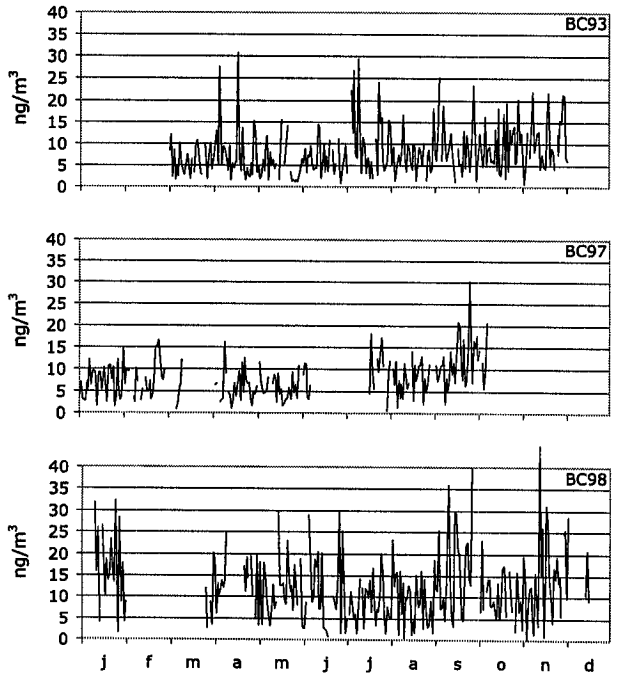

Figure 6. Daily averages of BC concentrations obtained at King George Island in the measurements years of 1993, 1997, and 1998.

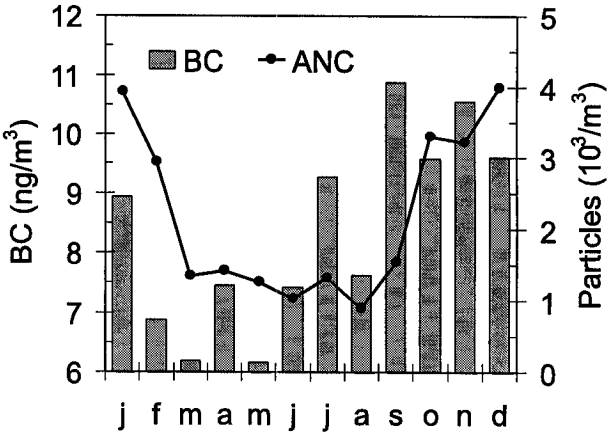

Figure 7. Mean monthly averages of BC concentrations during 1993–1998 period and ANC during 1997 obtained at King George Island.

[38] The increase of BC concentration during the summer can be explained by a local effect linked to the increase of human activities in King George Island corresponding to the increase in logistic operations and maintenance in all stations. The small peak observed by the end of November in Ferraz station coincides with the arrival of the support vessel and by the arrival of the new station's team. During this period, intense circulation of motorized vehicles, boats, and helicopters occurs. It is also during this period that the local population increases from the usually 13-member winter crew to a more than 40 people occupation during the summer mission period. ANC time series displays a more steady seasonal effect probably because the local manmade effects are less important than the increase of aerosols linked to the growth of bare terrain during summer or the decrease in the atmospheric aerosol load caused by the decrease in sea salt spray during winter.

5. Discussions

[39] The BC anomaly observed during the winter-to-spring period corresponds to the time of the year when considerable activity of burning biomass takes place in the whole Southern Hemisphere (Brazil, Africa, Australia, and Indonesia). Data from *Hansen et al.* [1988], *Wolff and Cachier* [1998], and Rolf Weller from the AWI Air Chemistry Observatory (http://www.awi-bremerhaven.de/) also reveal a similar anomaly for BC data collected in the Antarctic Plateau.

[40] In order to validate the winter-to-spring anomalous BC trend, we also performed SEM-EDS analysis for total carbon on filters returned from Ferraz, the same filters used on the aethalometer. The result is presented in Figure 8 along with those of the monthly averaged BC from several other Antarctic sites compiled from the literature. The winter-to-spring concentration growth was found as well as the season trend. The apparent shifts between the time series most probably result from the averaging process in the case of the continuous measurements and from the accumulation time during the filter

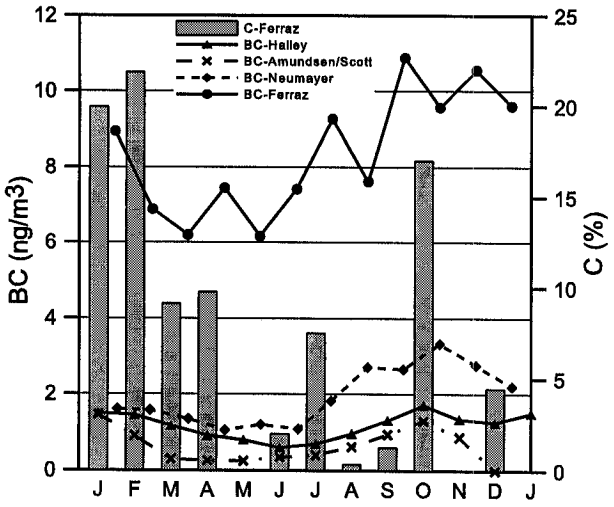

Figure 8. Comparison of BC (ng/m^3) and total carbon C (%) from Ferraz compared with data obtained from the literature for several stations in the Antarctic Peninsula and Antarctic Plateau. Data for Amundsen-Scott are from *Hansen et al.* [1988], for Halley from *Wolff and Cachier* [1998], and for Neumayer from the AWI Air Chemistry Observatory Web site (http://www.awi-bremerhaven.de).

collection, as in the case of the SEM-EDS. We believe that time shifts not exceeding 15–20 days can be considered acceptable and constitute a known limitation factor of the averaging and data handling techniques. BC concentrations in Ferraz are much higher, by a factor of 4–5, than what was found for the other stations, which is consistent with the decreasing latitudinal concentration trend presented in Figures 1 and 9, compiled from other authors.

[41] From a simulation of BC distribution by a global dispersion model as reported by *Penner et al.* [1993] and shown in Figure 9 (right) it is possible to follow the contour lines of BC isoconcentrations in ng m^{-3}. Source terms in her model included mostly urban centers and employed the relationship between SO_2 and BC to infer the desired BC isoconcentrations. In this simulation, the average values for BC in the area where Ferraz Station is located range between 1 and 10 ng m^{-3}, in accordance with the reference of 8.3 ng m^{-3} obtained from our annual mean for BC. This average was taken as a baseline in the interpretation and significance of anomalous data such as the case of the winter-to-spring anomaly in Ferraz.

[42] Figure 9 (left) presents a comparison between time series of BC measured at Ferraz and the numbers of fire pixels from burning biomass derived from NOAA satellite images for Brazil during the same period. This was achieved using images from the Advanced Very High Resolution Radiometer (AVHRR) aboard the NOAA-11 satellite, through its thermal channel 3 (3.55–3.93 mm). This technique is described in detail by *Setzer and Pereira* [1991b], and data is now routinely available at CPTEC (http://www.cptec.inpe.br/queimadas). The time lag in Figure 9 (left) between the peak of maximum burning biomass activity in Brazil and the peak of maximum observed BC at Ferraz is of 15 days, of the same order than the lifetime of BC in the atmosphere, between 6 and 10 days found by *Cooke and Wilson* [1996].

5.1. Meso- to Long-Range Transport of Black Carbon

[43] Figure 10 (left) depicts the wind vector fields for day 4 of the event shown in Figure 5, when radon reached perhaps its highest level. To better understand this process, we examined wind vector fields at 850 hPa from NCEP reanalysis [*Kalnay et al.*, 1996] and satellite pictures for the duration of this event. It illustrates the airflow from the tropical and subtropical region of South America southward, over east Bolivia and Paraguay, likely related to a low-level jet east of Andes. This jet intensified when the frontal system crossed the Drake Passage, and the southward winds extended from southern South America to the Antarctic Peninsula. Sea surface pressure fields (not shown) revealed the influence of the frontal system arrival over the Drake Passage and the high pressure over the Atlantic Ocean associated with the subtropical high. This low-level anticyclone circulation centered over South Atlantic is one of the most prominent features of the mean large-scale flow close to South America. It defines an airflow regime, which would ultimately be responsible for the continental outflow to the Atlantic Ocean also of the biomass burning products in the central areas of Brazil. *Pereira et al.* [1996] and *Anderson et al.* [1996], for example, have detected this outflow by instrumented aircraft flights during TRACE-A experiment in 1992, in the southern region of Brazil north of Uruguay. In the present study, the low-pressure area associated with the cyclonic circulation seen on the satellite image of Figure 10 (right) extend northward as the frontal system displaces eastward. The configuration of low and high pressure is consistent with an effective irregular flow directed meridionally from continental areas southward. This synoptic condition is favorable to the transport of air masses from tropical continental areas southward to Antarctic latitudes. Another synoptic feature that could contribute to the biomass burning transport to higher latitudes is the frequent incursion of a middle or upper level trough over central South America in the austral winter. The biomass burning plumes that might ascend to high levels by some mechanism, such as by the thermal plumes caused by large forest fires, may be transported southward by the winds associated with this wave flow. Subsidence that can bring the material to low levels at higher latitudes can occur to the east of an upper-level ridge following the passage of a frontal system.

[44] It is likely that the air masses containing biomass-burning particles can be transported from South America to the Antarctic Peninsula by a combination of low-level flows explained in the previous paragraphs. As discussed in the previous case of ^{222}Rn, this feature can be identified in wind flow fields also for the events of biomass burning herein presented, as in the case shown in Figure 11, when the activities of burning biomass in Brazil were peaking. Considering that BC has a relatively long lifetime in the troposphere (between 6 and 10 days according to *Cooke and Wilson* [1996]), such a mechanism could also be responsible for the BC concentration increase reported in this paper.

[45] The corresponding BC event at Ferraz can be seen in Figure 12 showing the maximum BC on the 22nd when

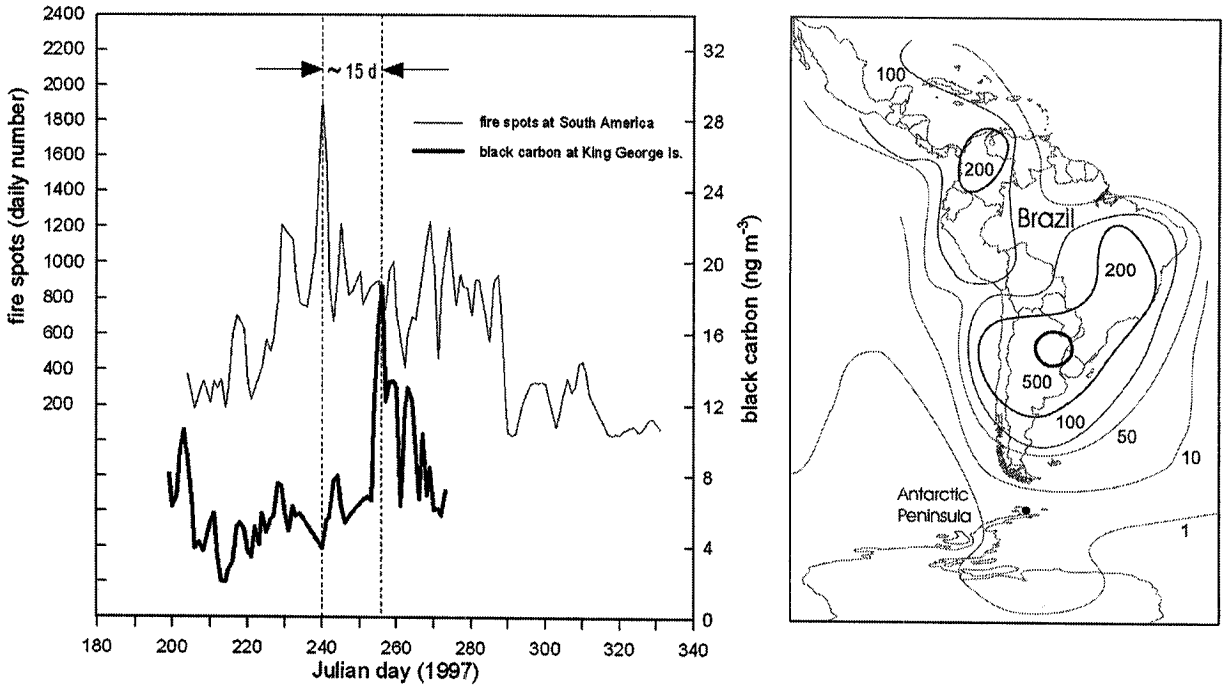

Figure 9. (left) BC and fire spot numbers monthly averages for the winter-to-spring; (right) a global dispersion model of BC with focus on Latin America-West Antarctic area (based on *Penner et al.* [1993]).

the wind fields were most favorable to the northerly transport form Brazil. Displacements of low-pressure systems over the Drake Passage and air circulation in the southwest Atlantic Ocean occasionally provide favorable conditions to the transport of BC from Central South America to the north of the Antarctica Peninsula. In the example of Figures 11 and 12, a low-pressure system moved eastward from the Pacific southeast Ocean, and

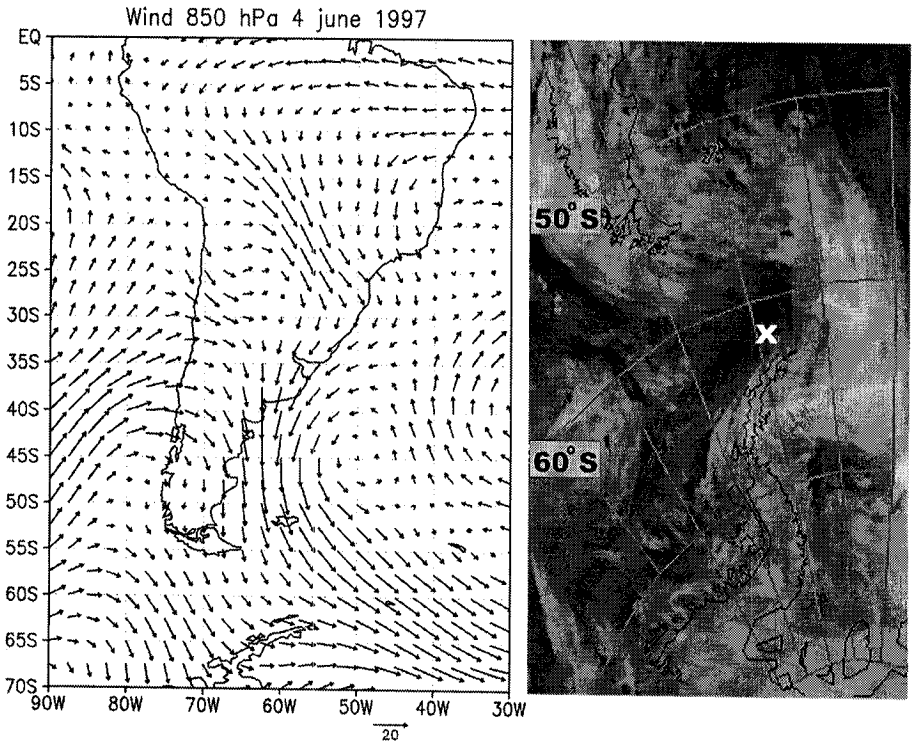

Figure 10. (left) Wind vectors at 850 hPa from NCEP reanalysis during 04/06/1997 and (right) NOAA 12 satellite image for the same day.

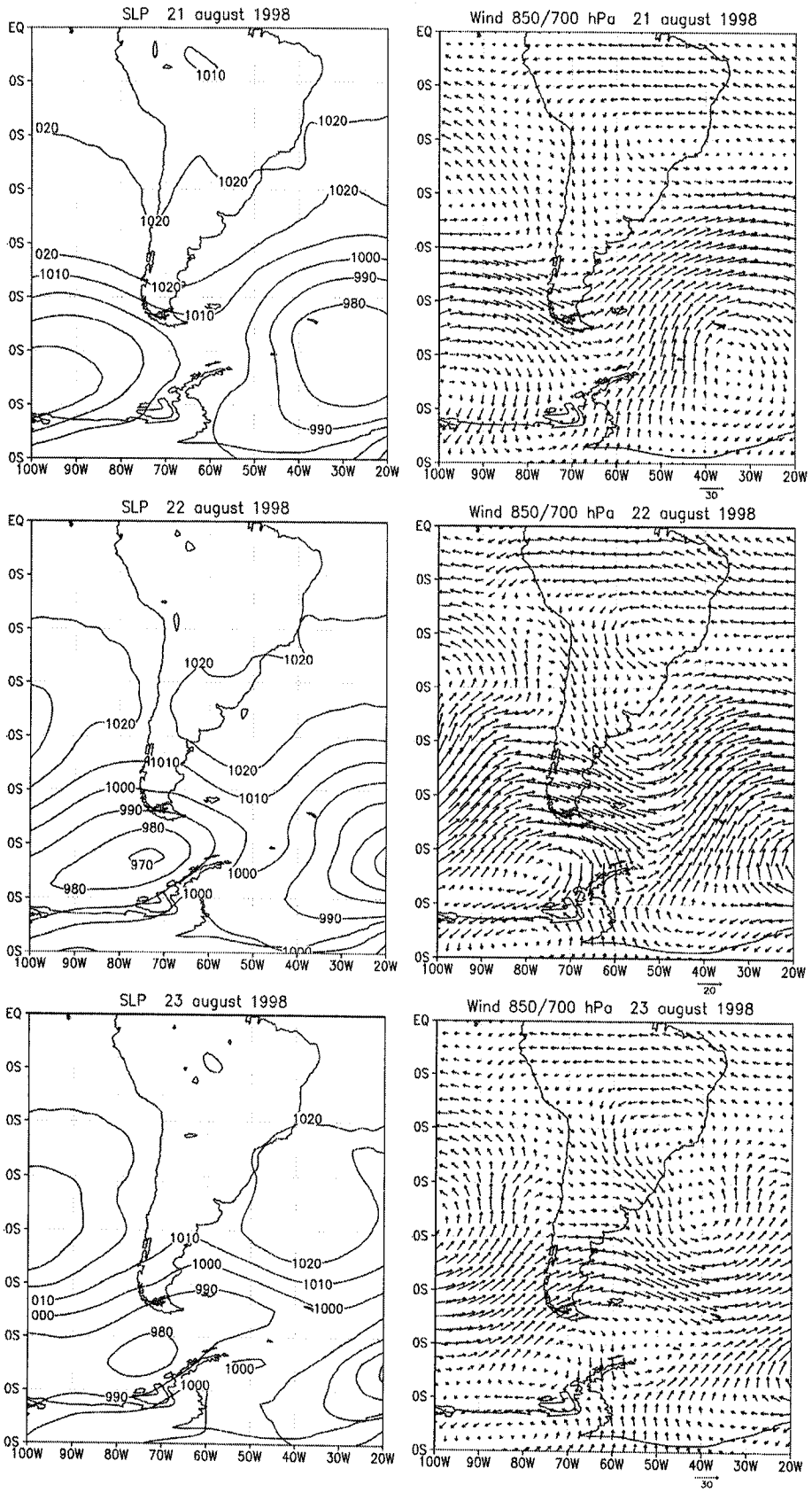

Figure 11. Pressure and wind field average in the layer 850 hPa to 700 hPa between 21 and 23 August 1998.

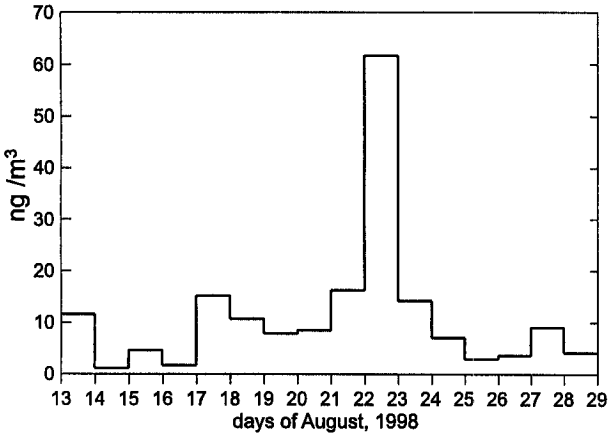

Figure 12. BC concentrations over Ferraz during a favorable condition for major low-level flow between South America and the Antarctic Peninsula.

strong southward winds from central Brazil could be noticed over east South America.

[46] Figure 13 shows a case study of the effective meridional wind component for the winter of 1998. During this season, the Amazonian region and central Brazil are sources of burning biomass particles. At 30°S, frequent and persistent northerly flow (negative meridional wind), mainly from 70°W to 50°W, indicates the outflow from the South America continent southward. This flow can transport burning particles from tropical to middle latitudes. When cyclonic systems cross Drake Passage, the northerly flow can transfer the burning particles to the Antarctica Peninsula. This feature is consistent with several periods of negative meridional wind at 60°S (Figure 13b) that indicates northerly flow to the Antarctica Peninsula.

5.2. Factor Analysis

[47] Factor Analysis was applied on our data to study the relationships between variables and to study the trace component signature of the air masses arriving in the Ferraz area. To reduce the number of variables and to detect structure in the relationships between variables, we used only data for 1997 because during this year we obtained the most continuous database. Data from the other acquisition periods were subjected to several gaps in one or more variables due to instrument problems or maintenance operations and were judged not suitable for the application of the Factor Analysis method. We have selected the following variables from our data set: black carbon (BC), radon concentration activity (^{222}Rn), air temperature (T_{air}), atmospheric pressure (P_{atm}), wind velocity (v), relative humidity (RH), aerosol particle number concentration (ANC), surface soil temperature (T_{surf}), and Thoron concentration activity (^{220}Rn). Table 1 shows the result of the extraction of the principal components and their respective factor loadings after the variance maximizing. Factor loadings greater than 0.5 were retained for discussion about trace-element signatures in air masses. Factor 1 links air temperature and soil temperature with the short-lived ^{220}Rn (half life of 55 s) and can be attributed to local emanation of ^{220}Rn by the ice melting when temperature gets higher than 0°C and the effect of ice-free areas become relevant. This is a frequent scenario during the austral summer in subpolar regions but occurs eventually even during the winter. Factor 2 links BC and ANC with no association with the meteorological parameters. This factor can be explained by local man-related activities. Such local contributions are of short duration and are responsible for surges of atmospheric aerosols above one order of magnitude higher than the annual average. Factor 3 links atmospheric pressure and wind velocity. Changes in wind velocity and atmospheric pressure in Ferraz are associated to the cyclonic systems (low pressure systems) that regularly travel through the Drake Passage. Factor 4 links ^{222}Rn and BC with the wind velocity, and can be attributed to meso-long range atmospheric transport. The BC observations extracted from this fourth factor are therefore linked to the ^{222}Rn, which has a definite land continental origin from South America [*Pereira*, 1990; *Pereira et al.*, 1988].

6. Conclusions

[48] BC concentrations measured in the Ferraz Antarctic station area in the northwest of the Antarctic Peninsula presented the highest values with respect to other Antarctic stations. The annual average value was 8.3 ng m^{-3}, for the years of 1993, 1997, and 1998. This average was consistent with the results of a global dispersion model by *Penner et al.* [1993] that mostly considers the BC burden from fossil fuel produced in urban areas worldwide. Raw data for BC at King George Island have shown several degrees of contamination by activities from local scientific stations. Therefore we developed and applied several procedures of BC data filtering based on visual inspection of data, relationship with ANC data, ^{222}Rn and wind direction simultaneous measurements, angular sector screening, and peak duration. These procedures were intended to remove most of local BC upsurges originated from the station's activities while preserving the regional and long-range information. Both BC and the ANC time series revealed a seasonal character with minimum values during the fall-winter seasons. Superimposed on the season minimum during winter, the BC and total C time series displayed relative increases in concentration during the winter-to-spring period, coinciding with the peak of biomass burning in central South America. ANC time series displays a more steady seasonal effect explained by the increase of aerosols linked to the expansion of exposed bare terrain during summer or the decrease in the atmospheric aerosol load caused by the decrease in sea salt spray during winter.

[49] Factor analysis applied to the variables BC, ANC, radon (^{222}Rn), thoron (^{220}Rn), air and soil temperature, atmospheric pressure, wind velocity, and relative humidity, revealed four principal component factors that control the variability of the data. The first factor for ^{222}Rn is regional and was associated to the variation in the extension of the ice-free area during summer. The second factor links BC and ANC and could be explained by local man-made activities. The third factor links atmospheric pressure with wind. Factor four links ^{222}Rn and BC with wind speed and could be explained by meso-long range atmospheric transport of these atmospheric components.

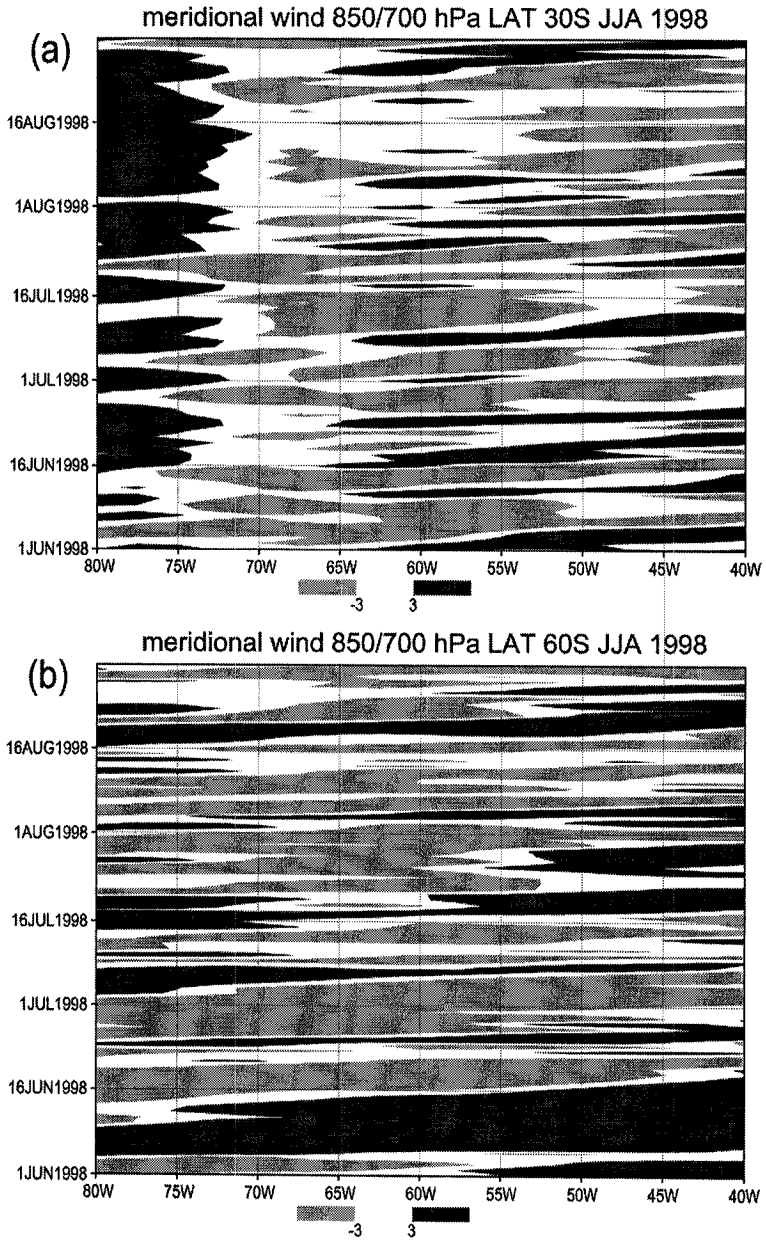

Figure 13. Daily meridional wind (m s^{-1}) in June, July, and August at (a) 30°S and (b) 60°S.

[50] The increase in BC and total C concentrations observed during the winter-to-spring period in the South Shetland Islands are most probably caused by not direct, nonlinear linkages between the south tropics and the Antarctic troposphere. The sources of BC are in areas of biomass burning that takes place routinely in central Brazil during the dry season (July to November). This linkage is triggered by the low-level anticyclone circulation centered over South Atlantic and leads to the mean large-scale continental outflow to the Atlantic Ocean. These outflows eventually combine with the intermittent cyclonic circulation over the extreme south of the South American continent. The intermittent nonlinear coupling mechanism between the circulation over central South America and

Table 1. Principal Component Analysis for Normalized Meteorological Data, ANC, BC, and Radon, Monitored During 1997 at Ferraz Station

	Factor Loadings-(Varimax Normalized) Principal Components			
Variables	Factor 1	Factor 2	Factor 3	Factor 4
^{222}Rn	0.397	−0.490	−0.329	**0.529**
^{220}Rn	**0.533**	−0.460	0.055	0.054
BC	−0.281	**0.571**	0.134	**0.565**
P_{atm}	0.113	0.059	**−0.830**	−0.035
RH	0.371	−0.483	0.438	−0.345
V	−0.021	−0.248	**0.515**	**0.589**
T_{air}	**0.810**	0.263	−0.249	0.167
T_{surf}	**0.864**	0.338	0.198	−0.010
ANC	0.408	**0.645**	0.271	−0.152

synoptic systems over the Drake Passage can ultimately explain the transport of BC to the Antarctic Peninsula.

[51] **Acknowledgments.** We gratefully thank the Brazilian Antarctic Program (PROANTAR/CNPq, PROANTAR- SECIRM and PROANTAR-MMA - Rede 1) for continuous logistical and financial (grants CNPq-6300017 and CNPq/MMA-550353/02) support. We also thank Juan Maldonado for the black carbon global data compilation and Marcelo Sampaio and Heber R. Passos for constant technical and maintenance support and the technical staff of INPE/DGE and LCR/UERJ and Ferraz Base group involved in the project.

References

Anderson, E. A., W. B. Grant, G. L. Gregory, E. V. Browell, J. E. Collins Jr., G. W. Sachse, D. R. Bagwell, C. H. Hudgins, and N. J. Blake (1996), Aerosols from biomass burning over the tropical South Atlantic region: Distribution and impacts, *J. Geophys. Res.*, *101*(D19), 24,117–24,137.

Artaxo, P., E. T. Fernandes, J. M. Martins, M. A. Yamasoe, P. T. Hobbs, W. Maenhaut, K. M. Longo, and A. Castanho (1998), Large-scale aerosol source apportionment in Amazonia, *J. Geophys. Res.*, *103*(D24), 31,837–31,848.

Basile, I., F. E. Grousset, M. Revel, J. R. Petit, P. E. Biscaye, and N. Barkov (1997), Patagonian origin of glacial dust deposited in the east Antarctica (Vostok and Dome C) during glacial stages 2, 4 and 6, *Earth Planet. Sci. Lett.*, *146*, 573–589.

Battye, W., K. Boyer, and T. G. Pace (2002), Methods for improving global inventories of black carbon and organic carbon particulates, paper presented at 11th International Emission Inventory Conference, U.S. Environ. Prot. Agency, Atlanta, Ga.

Brian, M., A. Royer, R. Petit, and C. Lorius (1982), Late glacial input of aeolian continental dust in the Dome C ice core: Additional evidence from individual microparticle analysis, *Ann. Glaciol.*, *3*, 27–30.

Cooke, W., and J. Wilson (1996), A global black carbon aerosol model, *J. Geophys. Res.*, *101*(D14), 19,395–19,410.

Correia, A. L. (1998), Atmospheric aerosols in Antarctica: Season trends, elemental composition and relationships with El Niño (in Portuguese), M.S. thesis, Inst. of Phys., Univ. of São Paulo, São Paulo, Brazil.

Evangelista, H. (1998), The use of radon for characterization of transport phenomena and environmental impacts in the atmosphere of King George Island, Antarctica (in Portuguese), Ph.D. thesis, Inst. of Biol. "Roberto Alcântara Gomes," State Univ. of Rio de Janeiro, Rio de Janeiro, Brazil.

Evangelista, H., and E. B. Pereira (1994), Critical analysis in remote stations for atmospheric aerosol studies, (in Portuguese), paper presented at Latin American Conference on Space and Atmospheric Sciences in Antarctic, Braz. Antarct. Progr. (PROANTAR), Serra Negra, São Paulo, Brazil.

Evangelista, H., and E. B. Pereira (2002), Radon flux at King George Island, Antarctic Peninsula, *J. Environ. Radioactivity*, *61*, 283–304.

Fishman, J., C. E. Watson, J. C. Larsen, and J. A. Logan (1990), Distribution of tropospheric ozone determined from satellite data, *J. Geophys. Res.*, *95*, 3599–3617.

Hansen, J., and L. Nazarenko (2004), Soot climate forcing via snow and ice albedoes, *Proc. Natl. Acad. Sci.*, *101*(2), 423–428, doi:10.1073/pnas.2237157100.

Hansen, A. D. A., and R. C. Schnell (1991), The aethalometer, *Open File Rep.*, p. 83, Magee Sci., Berkeley, Calif.

Hansen, A. D. A., B. A. Bodhaine, E. G. Dutton, and R. C. Schnell (1988), Aerosol black carbon measurements at the South Pole: Initial results, 1986–1987, *Geophys. Res. Lett.*, *15*, 1193–1196.

Intergovernmental Panel on Climate Change (2001), *Climate Change 2001: The Scientific Basis*, edited by J. T. Houghton et al., Cambridge Univ. Press, New York.

Jacob, D. J., et al. (1997), Evaluation and intercomparison of global atmospheric transport models using ^{222}Rn and other short-lived tracers, *J. Geophys. Res.*, *102*(D5), 5953–5970.

Jacobson, M. Z. (2002), Control of fossil-fuel particulate black carbon and organic matter, possibly the most effective method of slowing global warming, *J. Geophys. Res.*, *107*(D19), 4410, doi:10.1029/2001JD001376.

Kalnay, E., et al. (1996), The NCEP/NCAR 40-year reanalysis project, *Bull. Am. Meteorol. Soc.*, *77*, 437–471.

Karoly, D. K., D. G. Vincent, and J. M. Schrage (1999), General circulation, in *Meteorology of the Southern Hemisphere*, *Meteorol. Monogr. Ser.*, vol., 27, edited by D. J. Karoly and D. G. Vincent, pp. 47–85, Am. Meteorol. Soc., Boston, Mass.

Kirkevag, A., T. Iversen, and A. Dahlback (1999), On radiative effects of black carbon and sulphate aerosols, *Atmos. Environ.*, *33*, 2621–2635.

Liousse, C., H. Cachier, and S. G. Jennings (1993), Optical and thermal measurements of back carbon content in different environments: Variation of the specific attenuation cross-section, Sigma [σ], *Atmos. Environ.*, *27*(A), 1203–1211.

Maldonado, J. (2003), Elemental carbon as atmospheric tracer in the axis Rio – S. Paulo, (in Portuguese), M.S. thesis, Inst. of Biol. "Roberto Alcântara Gomes," State Univ. of Rio de Janeiro, Rio de Janeiro, Brazil.

Maring, H., and G. A. Schwartz (1994), Condensation particle counter for long-term continuous use in the remote marine environment, *Atmos. Environ.*, *28*(20), 3293–3298.

Martins, V. M., P. Artaxo, C. Liousse, J. S. Reid, P. V. Hobbs, and Y. J. Kaufman (1998), Effects of blck carbon content, particle size, and mixing on light absorption by aerosol from biomass burning in Brazil, *J. Geophys. Res.*, *103*(D4), 32,041–32,050.

Muñoz, J., A. M. Felícimo, F. Cabezas, A. B. Burgaz, and I. Martínez (2004), Wind as a long-distance dispersal vehicle in the Southern Hemisphere, *Science*, *304*, 1144–1147.

Murphey, B. B., and A. W. Hogan (1992), Meteorological transport of continental soot to Antarctica, *Geophys. Res. Lett.*, *19*(1), 33–36.

Penner, J., and S. Y. Zhang (2003), Soot and smoke aerosol may not warm climate, *J. Geophys. Res.*, *108*(D21), 4657, doi:10.1029/2003JD003409.

Penner, J. E., H. Eddleman, and T. Novakov (1993), Towards the development of a global inventory for elemental carbon emissions, *Atmos. Environ.*, *27*(A), 1277–1295.

Pereira, E. B. (1990), Radon-222 time series measurements in the Antarctic Peninsula [1986–1987], *Tellus*, *42*(B1), 39–45.

Pereira, E. B., A. W. Setzer, and I. F. A. Cavalcanti (1988), Radon-222 in the Antarctic Peninsula during 1986, *Radiat. Prot. Dosimetry*, *24*(1/4), 85–88.

Pereira, E. B., A. Setzer, F. Gerab, P. E. Artaxo, M. C. Pereira, and G. Monroe (1996), Airborne Measurements of biomass burning aerosols in Brazil related to the "TRACE-A" experiment, *J. Geophys. Res.*, *101*(D19), 23,983–23,992.

Pereira, K. C. D. (2002), Identification of transport events by use of micro-analyses in the atmosphere and in the glacial deposit, M.S. thesis, Inst. of Biol. "Roberto Alcântara Gomes," State Univ. of Rio de Janeiro, Rio de Janeiro, Brazil.

Pereira, K. C. D., H. Evangelista, E. B. Pereira, J. C. Simões, E. Johnson, and L. R. Melo (2004), Transport of crustal microparticles from Chilean Patagonia to the Antarctic Peninsula by SEM-EDS analysis, *Tellus, Ser. B*, *56*, 262–275.

Petit, J. R., U. Ezat, N. I. Barkov, and V. N. Petrov (1983), Identification of quartz microparticles in 20,000 BP Antarctic ice samples: a signature of last glacial environment, *Scanning Electr. Microsc.*, *4*, 1627–1633.

Satheesh, S. K., and V. Ramanathan (2000), Large differences in tropical aerosol forcing at the top of the atmosphere and Earth's surface, *Nature*, *405*, 60–63.

Sato, M., J. Hansen, D. Koch, A. Lacis, R. Rudey, O. Dubovik, B. Holben, M. Chin, and T. Novakov (2003), Global atmospheric black carbon inferred from AERONET, *Proc. Natl. Acad. Sci.*, *100*, 6319–6324, doi:10.1073/pnas.0731897100.

Schwerdtfeger, W. (1970), The climate of the Antarctic, in *Climates of the Polar Regions*, *World Surv. of Climatol.*, vol. 14, pp. 253–355, edited by S. Orvig, Elsevier, New York.

Setzer, A. W., and M. C. Pereira (1991a), Amazonia biomass burnings in 1987 and an estimate of their tropospheric emissions, *Ambio*, *20*(1), 19–22.

Setzer, A. W., and M. C. Pereira (1991b), Operational detection of fires in Brazil with NOAA/AVHRR, paper presented at International Symposium on Remote Sensing and Environment, CELPER, Rio de Janeiro, Brazil.

Simões, J. C., U. F. Bremer, F. E. Aquino, and F. A. Ferron (1999), Morphology and variations of glacial drainage basins in the King George Island ice field, Antarctica, *Ann. Glaciol.*, *29*, 220–224.

Smith, J., D. Vance, R. A. Kemp, C. Archer, P. Toms, M. King, and M. Zárate (2003), Isotopic constraints on the source of Argentinian loess with implications for atmospheric circulation and the provenance of Antarctic dust during recent glacial maxima, *Earth Planet. Sci. Lett.*, *2*(1), 181–196.

Warren, S. G., and A. D. Clarke (1990), Soot in the atmosphere and snow surface of Antarctica, *J. Geophys Res.*, *95*(D2), 1811–1816.

Wolff, E. W., and H. Cachier (1998), Concentration and seasonal cycle of black carbon in aerosols at a coastal Antarctic station, *J. Geophys. Res.*, *103*(D9), 11,033–11,041.

I. F. A. Cavalcanti, E. B. Pereira, and A. W. Setzer, Center for Weather Forecasts and Climate Studies, National Institute for Space Science, 12630-000 Cachoeira Paulista, SP, Brazil. (eniobp@cptec.inpe.br)

H. Evangelista and K. C. D. Pereira, Laboratory of Radioecology and Global Change, State University of Rio de Janeiro, CEP 20 550-013 Rio de Janeiro, RJ, Brazil.